Cerrahpaşa Med J 2023; 47(2): 135-140 ORIGINAL ARTICLE

Role of Diffusion-Weighted Magnetic Resonance Imaging in Assessment of Liver Injury After Radioembolization

Emine Şebnem Durmaz[1], Deniz Alış[2], Ahmet Baş[3], Sertaç Asa[4], Sait Sager[4], Fatih Gülşen[3]

[1]Department of Radiology, İstanbul University-Cerrahpaşa, Cerrahpaşa Faculty of Medicine, İstanbul, Turkey
[2]Department of Radiology, Acıbadem Mehmet Ali Aydınlar University Faculty of Medicine, İstanbul, Turkey
[3]Department of Interventional Radiology, İstanbul University-Cerrahpaşa, Cerrahpaşa Faculty of Medicine, İstanbul, Turkey
[4]Department of Nuclear Medicine, İstanbul University-Cerrahpaşa, Cerrahpaşa Faculty of Medicine, İstanbul, Turkey

Cite this article as: Durmaz EŞ, Alış D, Baş A, Asa S, Sager S, Gülşen F. Role of diffusion-weighted magnetic resonance imaging in assessment of liver injury after radioembolization. *Cerrahpaşa Med J.* 2023;47(2):135-140.

Abstract

Objective: We aimed to investigate the diagnostic value of diffusion-weighted imaging in assessing liver injury after radioembolization via comparing pre- and post-treatment apparent diffusion coefficient values of nontumoral liver parenchyma in patients who underwent radioembolization.

Methods: We retrospectively examined the apparent diffusion coefficient values of the nontumoral liver parenchyma in 21 patients who underwent radioembolization. The observers placed the ellipsoid region of interest onto the nontumoral liver parenchyma using diffusion-weighted images, and then these regions of interest were transferred to apparent diffusion coefficient maps. The paired *t*-test was used to compare the change between pre- and post-treatment apparent diffusion coefficient values of the treated and the contralateral liver lobe.

Results: The mean apparent diffusion coefficient value of the treated lobe was 1079.416 ± 194.57 mm^2/s before and 963.10 ± 171.87 mm^2/s after the treatment. A significant difference was observed between pre- and post-treatment mean apparent diffusion coefficient values of the treated lobe ($P = .001$). The mean apparent diffusion coefficient value of the contralateral lobe was 1114.24 ± 110.63 mm^2/s before and 1116.20 ± 96.52 mm^2/s after the treatment. No difference was observed between pre- and post-treatment mean apparent diffusion coefficient values of the contralateral lobe ($P = .057$).

Conclusion: We observed reduced apparent diffusion coefficient values in the treated lobe of the liver, and our results suggest that reduced apparent diffusion coefficient values might reflect liver injury secondary to radioembolization.

Keywords: Radioembolization, diffusion-weighted imaging, apparent diffusion coefficients, liver, hepatotoxicity

Introduction

External beam radiation therapy (EBRT) could efficiently destroy tumors of the liver regardless of their origin. However, normal liver parenchyma has also very low tolerance to radiation, and parenchymal injury is inevitable after EBRT. The liver disease after EBRT, known as radiation-induced liver disease, is a well-defined complication.[1,2] Intra-arterial radioembolization (RE) with yttrium-90 (Y-90)-embedded microspheres is a novel minimally invasive treatment method, which is being extensively used for unresectable primary liver malignancies or chemorefractory hepatic metastases.[3] Normal liver parenchyma is primarily supplied by the portal vein, while primary and secondary hepatic malignancies are preferentially vascularized by the hepatic arterial system.[4] Given the vascular supply of the tumors, Y-90 microspheres which are given into the relevant hepatic artery almost exclusively are delivered to the tumor while relatively sparing surrounding nontumoral liver parenchyma. However, the distribution of Y-90 microspheres in the relevant hepatic lobe depends on the density of the capillary. In cases of hypovascular tumors, the degree of distribution of Y-90 microspheres in nontumoral liver parenchyma will increase compared to cases of hypervascular tumors. Unfortunately, despite this highly selective route of the delivery, nontumoral liver parenchyma is exposed to a certain dose of radiation, and some patients show clinical and laboratory signs of hepatotoxicity after the RE treatment.[5] Liver diseases secondary to RE, namely radioembolizati on-induced liver disease (REILD), have been reported in several studies.[6-12] Radioembolization-induced liver disease is clinically characterized by jaundice and ascites appearing 1-2 months after the Y-90 RE treatment in the absence of tumor progression or bile duct occlusion. The main pathological change in these patients is consistent with veno-occlusive disease (VOD), which is characterized by sinusoidal congestion, atrophy, bleeding, and necrosis with phlebosclerotic lesions of the central veins.[13-15] Currently, there is no established method to identify pathological changes of disease before the clinical symptoms of REILD appear. Moreover, we have no knowledge regarding whether the patients without any clinical or biochemical signs of REILD also have pathological changes after the treatment. Hence, a non-invasive modality to assess potential pathological alterations in the liver parenchyma after the treatment is highly desirable.

Diffusion-weighted imaging (DWI) is a magnetic resonance imaging (MRI) method, which is able to quantitatively measure the extracellular movement of the water, namely Brownian motion, by applying apparent diffusion coefficients (ADCs). In the current decade, liver DWI has seen an exponential increase in popularity and clinical applicability, and DWI has been increasingly used for

Received: August 15, 2022 **Accepted:** January 30, 2023
Publication Date: August 22, 2023
Corresponding author: Emine Şebnem Durmaz, Department of Radiology, İstanbul University-Cerrahpaşa, Cerrahpaşa Faculty of Medicine, Istanbul, Turkey **e-mail:** sebnem_memis@hotmail.com
DOI: 10.5152/cjm.2023.22066

assessing diffuse or focal liver pathologies.[16-26] The feasibility and accuracy of DWI in assessing liver fibrosis has been demonstrated in several studies.[16-23] However, to our knowledge, no single study exists, which has investigated the role of DWI in assessing potential liver injury after RE treatment.

In this study, we aimed to investigate the diagnostic value of DWI in assessing liver injury after RE via measuring and comparing pre- and post-treatment ADC values of nontumoral liver parenchyma in patients who underwent RE for secondary hepatic malignancies.

Methods

Patient Population

The local ethics committee of İstanbul University-Cerrahpaşa, Cerrahpaşa School of Medicine approved this retrospective single-center study, which was conducted between January 2018 and January 2021 (Date: August 8, 2018, Number: 40695). Informed consent was not required for retrospective review of the medical and radiological data of the patients. We reviewed our database for patients who underwent RE for secondary hepatic malignancies in our institute. Patients who had pre- and post-resonance imaging (RE) MRI including DWI sequences within 1 month prior to treatment and at an interval of 2-4 months after the treatment were included in the study. Exclusion criteria were having a chronic liver disease, MR images with significant motion or magnetic susceptibility artifacts, MR images with low contrast-to-noise ratio preventing interpretation of the images, and any history of previous local liver-directed interventional therapies including RE, transarterial chemoembolization, and radiofrequency ablation.

Magnetic Resonance Imaging Acquisition

Both pre- and post-procedural MRI were performed by the same 1.5 T MRI unit (Avanto Tim®, Siemens Healthcare, Forchheim, Germany) using a phased-array body coil. To ensure the reliability of the measurements, all MRIs were performed with the same device since ADC values were significantly affected by gradient linearity.[27] Our standard MRI protocol consisted of pre-contrast axial T1-weighted (T1W) and T2-weighted (T2W) sequences, pre-contrast coronal T2W sequence, post-contrast axial T1W sequences, and diffusion-weighted sequences. Diffusion-weighted imaging was performed using echo planar imaging in the axial plane using the following parameters: repetition time/echo time = 3500/75 ms, bandwidth = 1736 kHz, number of channels = 16, slice thickness = 5 mm, time of acquisition = 1.51 s, and range of field of view = 400, with *b*-values of 0 and 800 s/mm^2. Apparent diffusion coefficient maps were generated with voxel-by-voxel basis using the following equitation: ADC (mm^2/s) = $[\ln(S^0/S^b)]/b$ in which S^0 and S^b represent the signal intensities of the images with different gradient *b* factors, and *b* is the difference between gradient *b* factors.

Radioembolization Procedure

The decision of RE was made by a multidisciplinary tumor review board, which was attended by interventional radiologists, body radiologists, radiation therapists, hepatobiliary surgeons, oncologists, and nuclear medicine specialists. This tumor review board made their decisions in conjunction with previously described criteria for RE.[28]

All RE procedures were performed by 2 interventional radiologists with more than 15 years of experience in interventional radiology. Diagnostic catheter angiography and both planar and single photon emission computed tomography following an intra-arterial injection of 200-400 MBq of 99mTc-macroaggregated albumin were utilized to detect the percentage of pulmonary and intra-abdominal shunting. Aberrant vessels arising from the relevant hepatic artery were embolized using coils to impede non-target embolization. Radioembolization treatment was utilized within the following 2 weeks after the catheter angiography. Yttrium-90 microspheres (TheraSphere; BTG, London, England) were given into appropriate branches of the hepatic artery. The body surface area method was used to calculate the administered activity of Y-90 microspheres.[29]

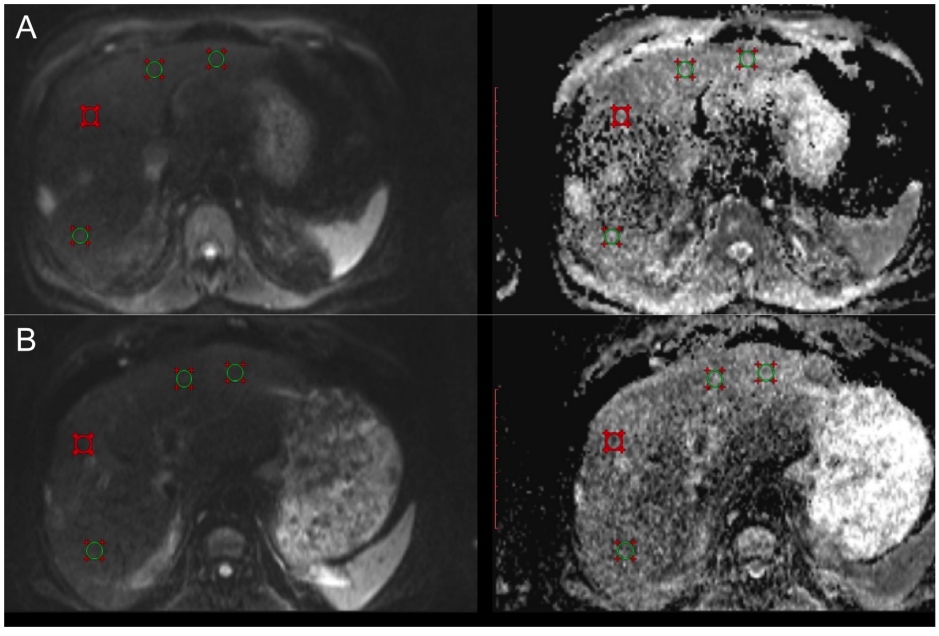

Figure 1. Axial diffusion-weighted images and apparent diffusion coefficient (ADC) maps images at *b* values of 800 s/mm^2 in a patient with right lobe colorectal liver metastases. (A) One month prior to RE treatment of the right lobe (mean ADC value of the right lobe: 1150.36 mm^2/s, mean ADC value of the left lobe: 1248.8 mm^2/s). (b) Three months after RE treatment of the right lobe (mean ADC value of the right lobe: 1021.65 mm^2/s, mean ADC value of the left lobe: 1219.14 mm^2/s).

Image Interpretation

Two radiologists, blinded to all clinical data concerning the patients, with more than 5 years of experience in body radiology, performed all the measurements in a consensus. All measurements were performed using a dedicated workstation (Extreme workstation, ExtremePACS System, Ankara, Turkey). Apparent diffusion coefficient measurements of the nontumoral liver parenchyma were performed from 3 consecutive slices in the medial and lateral left lobe and the anterior and posterior right lobe of nontumoral liver parenchyma. First, the observers placed the ellipsoid regions of interest (ROIs) onto the nontumoral liver parenchyma using diffusion-weighted images with a *b* value of 0 s/mm^2 as a guide, and then these ROIs were automatically transferred to ADC maps. Care was taken to avoid vessels, biliary ducts, and focal liver lesions during the measurements. The measured area of ROI was set at approximately 1 cm^2. The observers place 1 ROI in the mentioned segments and performed measurements for the following 3 sections of the liver. The average ADC value was calculated and noted for the right and left lobes after the measurements. All images were achieved using our picture archiving and communication system (PACS, ExtremePACS System, Ankara, Turkey). Figure 1 depicts ADC measurements of the liver parenchyma step by step.

Table 1. Characteristics of the Patients

Demographics and Clinical Characteristics	Finding
Age (years)*	42.0 ± 11.38
Gender	
Male	10
Female	11
Primary tumor type	21
Colorectal carcinoma	9/21 (42.5%)
Cholangiocarcinoma	4/21 (19%)
Breast carcinoma	3/21 (14.3%)
Lung cancer	2/21 (9.5%)
Neuroendocrine tumor	1/21 (4.8%)
Medullary thyroid carcinoma	1/21 (4.8%)
Bladder cancer	1/21 (4.8%)
Presence of extrahepatic metastases	
No	16
Yes	5
Presence of ascites before the intervention	
No	17
Yes	4
Treated lobe of the liver	
Right lobe	16
Left lobe	3
*Sequential treatment of each lobe***	2
Previous systemic chemotherapy	
No	5
Yes	16
The mean administered activity/target volume (GBq/L)*	4.53 ± 2.47

*Values are expressed as mean ± SD.
**Sequential lobar treatment delivering partitioned doses to the right and left liver lobe at an interval of 4-6 weeks.

Statistical Analyses

Statistical analyses were performed using the Statistical Package for Social Sciences version 21.0 (IBM SPSS Corp.; Armonk, NY, USA). Descriptive analyses were presented using means and SDs. The variables were investigated using visual (histograms and probability plots) and analytical methods (Shapiro–Wilk test) to determine whether the variables were normally distributed or not. Pre- and postoperative ADC values and other continuous variables were compared using the paired *t*-test. A *P*-value less than .05 was accepted as significant. All variables were expressed as mean ± SD unless otherwise specified. The parameters affecting ADC changes were investigated using Spearman/Pearson correlation tests. A multiple linear regression model was used to identify independent predictors of ADC changes. The model fit was assessed using appropriate residual and goodness-of-fit statistics. A 5% type-1 error level was used to infer statistical significance.

Results

Finally, 21 patients (10 female and 11 male; mean age 61.52 years; age range 42-78 years) were included in the study. The detailed characteristics of the study cohort are summarized in Table 1, and detailed laboratory findings before and after the treatment are listed in Table 2. The mean ADC value of the treated lobe was 1079.416 ± 194.57 mm^2/s before and 963.10 ± 171.87 mm^2/s after the treatment. A significant difference was observed between pre- and post-treatment mean ADC values of the treated lobe (P = .001). The mean absolute ADC change was –123.90 ± 165.85 mm^2/s, and the relative ADC change was –10.64%. The mean ADC value of the contralateral lobe was 1114.24 ± 110.63 mm^2/s before and 1126.20 ± 96.52 mm^2/s

Table 2. Laboratory Findings of the Patients Before and After the RE Treatment

	Pre-treatment	Post-treatment	*P*
Total bilirubin (mg/dL)	0.56 ± 0.18	1.55 ± 3.10	.024
Creatinine (mg/dL)	0.67 ± 0.2	0.67 ± 0.21	NS
ALT (IU/L)	29.71 ± 0.3	16.54 ± 48.63	.001
AST (IU/L)	31.66 ± 24.57	60.57 ± 44.76	.001
Platelet count (10^3/mm^3)	257.28 ± 93.71	242.87 ± 96.24	NS
Albumin (g/dL)	3.80 ± 0.66	3.38 ± 0.9	.013
GGT (IU/L)	100.7 ± 47.86	115.7 ± 40.55	NS
International normalized ratio	1.05 ± 0.06	0.98 ± 0.05	.034
Leukocyte count (10^3/mm^3)	6571 ± 1672	5938 ± 1303	NS

ALT, alanine aminotransferase; AST, aspartate transaminase; GGT, gamma glutamyl transferase; NS, not significant RE, radioembolization.

Table 3. Mean Pre- and Post-radioembolization ADC Measurements of the Treated and Contralateral Lobes of the Tumor-Free Liver Parenchyma

	Pre-treatment	Post-treatment	Absolute ADC Difference	Relative ADC Difference	*P*
Treated lobe ADC values (mm^2/s)	1079.416 ± 194.57	963.10 ± 171.87	–123.90 ± 165.85	–10.64% ± 12.13	.001
Contralateral lobe ADC values (mm^2/s)	1114.24 ± 110.63	1126.20 ± 96.5	–25.27 ± 54.10	–2.14% ± 4.61	.057

All values are expressed as mean ± SD.
ADC, apparent diffusion coefficient.

Table 4. Multivariate Linear Regression Analyses of Factors on ADC Value Reduction

Variable	*P*	Beta
Age	.236	0.267
Gender	.962	0.012
History of previous chemotherapy	.697	–0.107
Administered activity	.213	0.351

ADC, apparent diffusion coefficient.

after the treatment. No difference was observed between pre- and post-treatment mean ADC values of the contralateral lobe (P = .057) (Table 3). Among 21 patients, none of the patients developed REILD. We also evaluated that the potential effect of age, gender, the amount of administered activity per target volume, and the existence of prior chemotherapy over ADC value decreases in the treated lobe of the liver after the RE using multiple linear regression analysis; however, we observed that none of these parameters affected nor correlated with decreased ADC values ($P > .05$) (Table 4).

Discussion

We demonstrated that nontumoral liver parenchyma's mean ADC value of the RE-treated lobe was significantly lower compared to the contralateral lobe. To our knowledge, we conducted the first study investigating the diagnostic value of the DWI for evaluating the liver injury after RE.

Though we did not have any pathological data regarding the nontumoral liver parenchyma, we suggest that several explanations for the reduced ADC values of the treated lobe's parenchyma could be proposed. First, to understand these potential mechanisms, we should briefly discuss the basic physical principles of DWI. Diffusion-weighted imaging could indirectly assess the composition of the tissues within the voxel by exploiting Brownian molecules of the protons, particularly protons. In tissues with high cellular concentration or with swollen cells, such as in tumors or acute ischemic stroke, or with increased amount of interstitial components, such as in fibrosis, the free random movement of the extracellular water is strictly restricted, and such tissues have bright signal on DWI and decreased ADC values on ADC maps. .[30-32]

Various morphological features were seen in patients' liver, which was partially absorbed at a dose of radiation over 30 Gray.[13-15] The main histological changes in these patients is VOD, and the typical pathologic findings of VOD are disruption of the hepatic microcirculation accompanied by extravasation of inflammatory cells into the sinusoidal space, subendothelial deposition of von Willebrand factor, and fibrinogen in central venules, as documented by several histological studies.[33-37] Moreover, in some patients, portal tract crowding and also periportal fibrosis could be seen to a certain extent at the later periods during the recovery phase.[38] It is very obvious that all of the mentioned pathological changes related to VOD in the earlier periods after the treatment (first 4 months) and also fibrosis (generally after 4 months)[2-39] would impede free diffusion of the water molecules, which eventually leads to restricted diffusion and reduced ADC values. We performed all follow-up MRIs at an interval of 2-4 months after the treatment; thus, which factors played the dominant role in the reduced ADC values could not be exactly inferred from our results. Moreover, we should admit that all of the previous pathological studies focused on patients with REILD; hence, the link between the reduced ADC values and these potential pathological alterations are only assumptions. However, an experimental animal study by Dong et al.[40] also documented reduced ADC values in rabbits exposed to radiation injury in which alterations suggested that VOD was demonstrated histopathologically, which is in line with our findings and assumptions. Overall, our preliminary work must be interpreted with caution and should be taken as providing evidence that requires validation with histological findings in a larger patient cohort.

The natural course of REILD/hepatotoxicity after RE has a broad variation; it can either be transient and self-limiting or result in fulminant hepatic failure and death. Also, as a late complication of RE and REILD, portal hypertension is increasingly being reported.[39,41-43] Radioembolization treatment is generally commenced in a sequential manner rather than the whole lobe treatment sessions, and there is usually an interval of weeks between 2 RE therapy sessions.[8] Currently, there is no recommended imaging modality for the evaluation of the liver parenchyma status, which is already hampered by the previous RE or systemic chemotherapy. We suggest that predicting the early pathological changes using DWI after RE, even before any clinical symptoms of hepatotoxicity appear, might play an important role in helping the physicians to individually select and form best therapy options for the patient.

Researchers have found several risk factors for liver injury after RE and REILD.[6,9,12,44-48] Liver-directed treatments such as pre-RE or post-RE chemotherapy,[6,9,45,47] history of previous RE[46] or other intraarterial therapies,[47] and preexisting chronic liver disease have been associated with increased risk of liver injury after RE.[48] Furthermore, the amount of activity administered relative to the total volume was described as an independent risk factor. Alzugaray et al[9] described activity per target volume as a significant risk factor for REILD, which occurs in most patients with a dose of higher than 0.8 GBq/L. However, in the present study, neither a history of previous chemotherapy nor radiation activity per target volume was associated with the ADC value decrease of the treated lobe. We believe that a small number of participants might have caused our inconsistent results with the previous literature.

We had several limitations in the present study. The first, and foremost, limitation was the retrospective study design. Hence, we could not obtain histopathological data to compare and confirm our radiological findings. However, in our study, no identifiable factor occurred in or was utilized for the patients, which could

have led to hepatotoxicity or pathological changes in the interval between the treatment and follow-up MRI. So, although the adverse effects of Y-90 in cases with chronic liver disease are clinically important, we excluded the cases having chronic liver disease. Because among the cases with chronic liver disease, reduced ADC values may also occur due to progression of cirrhosis. Thus, we assume that reduced ADC values were most likely to have occurred given the treatment. Second, since the present study is a single-center study with strict inclusion criteria, the patient population was relatively small to investigate the association between multiple risk factors and the alterations of ADC values. Prospective randomized trials with larger populations are needed to set up a more certain conclusion. Third, we did not give the correlation between the degree of ADC value decrease and the changes of blood tests such as bilirubin, alanine aminotransferase, aspartate transaminase, and albumin. In cases of progression of the tumor or bile duct occlusion, the laboratory values do not reflect the liver injury related to RE treatment on nontumoral liver parenchyma.

Conclusion

In conclusion, we demonstrated that ADC values of the liver lobe undergoing Y-90 RE showed a considerable reduction after the treatment; though not histopathologically proven, we suggest that these changes might reflect hepatotoxicity secondary to embolization procedure. We highlight that DWI may represent an important clinical tool for the prediction of liver injury after RE, yet more comprehensive works with histopathological data are needed to confirm our results.

Ethics Committee Approval: Ethical committee approval was received from the Ethics Committee of İstanbul University-Cerrahpaşa, Cerrahpaşa School of Medicine (Date: August 8, 2018, Number: 40695).

Informed Consent: Informed consent was not required for retrospective review of the medical and radiological data of the patients.

Peer-review: Externally peer-reviewed.

Author Contributions: Concept – E.Ş.D.; Design – E.Ş.D., D.A.; Supervision – A.B., F.G.; Resources – E.Ş.D., D.A.; Materials – E.Ş.D., A.B., S.A., S.S.; Data Collection and/or Processing – E.Ş.D., D.A.; Analysis and/or Interpretation – E.Ş.D., D.A., S.S., S.A., A.B., F.G.; Literature Search –E.Ş.D., D.A.; Writing Manuscript – E.Ş.D., D.A.; Critical Review – A.B., F.G.; Other – S.A., S.S.

Declaration of Interests: The authors have no conflict of interest to declare.

Funding: The authors declared that this study has received no financial support.

References

1. Lawrence TS, Robertson JM, Anscher MS, Jirtle RL, Ensminger WD, Fajardo LF. Hepatic toxicity resulting from cancer treatment. *Int J Radiat Oncol Biol Phys*. 1995;31(5):1237-1248. [CrossRef]
2. Sempoux C, Horsmans Y, Geubel A, et al. Severe radiation-induced liver disease following localized radiation therapy for biliopancreatic carcinoma: activation of hepatic stellate cells as an early event. *Hepatology*. 1997;26(1):128-134. [CrossRef]
3. Bester L, Meteling B, Pocock N, et al. Radioembolization versus standard care of hepatic metastases: comparative retrospective cohort study of survival outcomes and adverse events in salvage patients. *J Vasc Interv Radiol*. 2012;23(1):96-105. [CrossRef]
4. Bierman HR, Byron RL Jr, Kelley KH, Grady A. Studies on the blood supply of tumors in man. III. Vascular patterns of the liver by hepatic arteriography in vivo. *J Natl Cancer Inst*. 1951;12(1):107-131.
5. Sangro B, Iñarrairaegui M, Bilbao JI. Radioembolization for hepatocellular carcinoma. *J Hepatol*. 2012;56(2):464-473. [CrossRef]
6. Sangro B, Gil-Alzugaray B, Rodriguez J, et al. Liver disease induced by radioembolization of liver tumors: description and possible risk factors. *Cancer*. 2008;112(7):1538-1546. [CrossRef]
7. Rühl R, Seidensticker M, Peters N, et al. Hepatocellular carcinoma and liver cirrhosis: assessment of the liver function after yttrium-90 radioembolization with resin microspheres or after CT-guided high-dose-rate brachytherapy. *Dig Dis*. 2009;27(2):189-199. [CrossRef]
8. Seidensticker R, Seidensticker M, Damm R, et al. Hepatic toxicity after radioembolization of the liver using (90)Y-microspheres: sequential lobar versus whole liver approach. *Cardiovasc Intervent Radiol*. 2012;35(5):1109-1118. [CrossRef]
9. Gil-Alzugaray B, Chopitea A, Iñarrairaegui M, et al. Prognostic factors and prevention of radioembolization-induced liver disease. *Hepatology*. 2013;57(3):1078-1087. [CrossRef]
10. Fernandez-Ros N, Iñarrairaegui M, Paramo JA, et al. Radioembolization of hepatocellular carcinoma activates liver regeneration, induces inflammation and endothelial stress and activates coagulation. *Liver Int*. 2015;35(5):1590-1596. [CrossRef]
11. Zarva A, Mohnike K, Damm R, et al. Safety of repeated radioembolizations in patients with advanced primary and secondary liver tumors and progressive disease after first selective internal radiotherapy. *J Nucl Med*. 2014;55(3):360-366. [CrossRef]
12. Bester L, Feitelson S, Milner B, Chua TC, Morris DL. Impact of prior hepatectomy on the safety and efficacy of radioembolization with yttrium-90 microspheres for patients with unresectable liver tumors. *Am J Clin Oncol*. 2014;37(5):454-460. [CrossRef]
13. Lewin K, Millis RR. Human radiation hepatitis. A morphologic study with emphasis on the late changes. *Arch Pathol*. 1973;96(1):21-26.
14. Fajardo LF, Colby TV. Pathogenesis of veno-occlusive liver disease after radiation. *Arch Pathol Lab Med*. 1980;104(11):584-588.
15. Fajardo LF. The pathology of ionizing radiation as defined by morphologic patterns. *Acta Oncol*. 2005;44(1):13-22. [CrossRef]
16. Kim T, Murakami T, Takahashi S, Hori M, Tsuda K, Nakamura H. Diffusion- weighted single-shot echoplanar MR imaging for liver disease. *AJR Am J Roentgenol*. 1999;173(2):393-398. [CrossRef]
17. Aubé C, Racineux PX, Lebigot J, et al. Diagnosis and quantification of hepatic fibrosis with diffusion weighted MR imaging: preliminary results. *J Radiol*. 2004;85(3):301-306. [CrossRef]
18. Koinuma M, Ohashi I, Hanafusa K, Shibuya H. Apparent diffusion coefficient measurements with diffusion-weighted magnetic resonance imaging for evaluation of hepatic fibrosis. *J Magn Reson Imaging*. 2005;22(1):80-85. [CrossRef]
19. Taouli B, Tolia AJ, Losada M, et al. Diffusion-weighted MRI for quantification of liver fibrosis: preliminary experience. *AJR Am J Roentgenol*. 2007;189(4):799-806. [CrossRef]
20. Luciani A, Vignaud A, Cavet M, et al. Liver cirrhosis: intravoxel incoherent motion MR imaging—pilot study. *Radiology*. 2008;249(3):891-899. [CrossRef]
21. Lewin M, Poujol-Robert A, Boëlle PY, et al. Diffusion-weighted magnetic reso- nance imaging for the assessment of fibrosis in chronic hepatitis C. *Hepatology*. 2007;46(3):658-665. [CrossRef]
22. Wang Y, Ganger DR, Levitsky J, et al. Assessment of chronic hepatitis and fibrosis: comparison of MR elastography and diffusion-weighted imaging. *AJR Am J Roentgenol*. 2011;196(3):553-561. [CrossRef]
23. Do RK, Chandarana H, Felker E, et alDiagnosis of liver fibrosis and cirrhosis with diffusion-weighted imaging: value of normalized apparent diffusion coefficient using the spleen as reference organ. *AJR Am J Roentgenol*. 2010;195(3):671-676. [CrossRef]
24. Watanabe H, Kanematsu M, Goshima S, et al. Staging hepatic fibrosis: comparison of gadoxetate disodium-enhanced and diffusion-weighted MR imaging—preliminary observations. *Radiology*. 2011;259(1):142-150. [CrossRef]
25. Girometti R, Esposito G, Bagatto D, Avellini C, Bazzocchi M, Zuiani C. Is water diffusion isotropic in the cirrhotic liver? A study with diffusion-weighted imaging at 3.0 Tesla. *Acad Radiol*. 2012;19(1):55-61. [CrossRef]
26. Inan N, Akhun N, Akansel G, Arslan A, Ciftçi E, Demirci A. Conventional and diffusion-weighted MRI of extrahepatic hydatid cysts. *Diagn Interv Radiol*. 2010;16(2):168-174. [CrossRef]
27. Kim S, Jain M, Harris AB, et al. T1 hyperintense renal lesions: characterization with diffusion-weighted MR imaging versus contrast-enhanced MR imaging. *Radiology*. 2009;251(3):796-807. [CrossRef]
28. Ahmadzadehfar H, Biersack HJ, Ezziddin S. Radioembolization of liver tumors with yttrium-90 microspheres. *Semin Nucl Med*. 2010;40(2):105-121. [CrossRef]

29. Lau WY, Kennedy AS, Kim YH, et al. Patient selection and activity planning guide for selective internal radiotherapy with yttrium-90 resin microspheres. *Int J Radiat Oncol Biol Phys*. 2012;82(1):401-407. [CrossRef]
30. Charles-Edwards EM, deSouza NM. Diffusion-weighted magnetic resonance imaging and its application to cancer. *Cancer Imaging*. 2006;6(1):135-143. [CrossRef]
31. Thoeny HC, De Keyzer F. Extracranial applications of diffusion-weighted magnetic resonance imaging. *Eur Radiol*. 2007;17(6):1385-1393. [CrossRef]
32. Kwee TC, Takahara T, Ochiai R, Nievelstein RA, Luijten PR. Diffusion-weighted whole-body imaging with background body signal suppression (DWIBS): features and potential applications in oncology. *Eur Radiol*. 2008;18(9):1937-1952. [CrossRef]
33. Shulman HM, Gown AM, Nugent DJ. Hepatic venoocclusive disease after bone marrow transplantation, immunohistochemical identification of the material within occluded central venules. *Am J Pathol*01. 1987;127(3):549-558.
34. Ailen JR, Carstens LA, Katagiri GJ. Hepatic veins of monkeys with veno-occlusive disease. Sequential ultrastructural changes. *Arch Path*. 1969;87;01:279-289.
35. Brooks SEH, Miller CG, McKenzie K, Audretsch JJ, Bras G. Acute venoocclusive disease of the liver: fine structure in Jamaican children. *Arch Pathol*. 1970;89(6):507-520.
36. Bicher HI, Dalrymple GV, Ashbrook D, Smith R, Harris D. Effect of ionizing radiation on liver microcirculation and oxigenation. *Adv Exp Med Biol*. 1976;75:497-503. [CrossRef]
37. Rio B, Andreu G, Nicod A, et al. Thrombocytopenia in venocclusive disease after bone marrow transplantation or chemotherapy. *Blood*. 1986;67(6):1773-1776.
38. DeLeve LD, Shulman HM, McDonald GB. Toxic injury to hepatic sinusoids: sinusoidal obstruction syndrome (veno-occlusive disease). *Semin Liver Dis*. 2002;22(1):27-42. [CrossRef]
39. Nalesnik MA, Federle M, Buck D, Fontes P, Carr BI. Hepatobiliary effects of 90yttrium microsphere therapy for unresectable hepatocellular carcinoma. *Hum Pathol*. 2009;40(1):125-134. [CrossRef]
40. Dong TM, Ma L, Zhou ZH, et al. Diagnosing radiation-induced liver injury in rabbit using 3.0 Tesla magnetic resonance diffusion-weighted imaging. *Zhonghua Gan Zang Bing Za Zhi*. 2014;22(2):128-135. [CrossRef]
41. Kuo JC, Tazbirkova A, Allen R, Kosmider S, Gibbs P, Yip D. Serious hepatic complications of selective internal radiation therapy with yttrium- 90 microsphere radioembolization for unresectable liver tumors. *Asia Pac J Clin Oncol*. 2014;10(3):266-272. [CrossRef]
42. Jakobs TF, Saleem S, Atassi B, et al. Fibrosis, portal hypertension, and hepatic volume changes induced by intraarterial radiotherapy with 90yttrium microspheres. *Dig Dis Sci*. 2008;53(9):2556-2563. [CrossRef]
43. Maleux G, Deroose C, Laenen A, et al. Yttrium-90 radioembolization for the treatment of chemorefractory colorectal liver metastases: technical results, clinical outcome and factors potentially influencing survival. *Acta Oncol*. 2016;55(4):486-495. [CrossRef]
44. Golfieri R, Bilbao JI, Carpanese L, et al. Comparison of the survival and tolerability of radioembolization in elderly vs. younger patients with unresectable hepatocellular carcinoma. *J Hepatol*. 2013;59(4):753-761. [CrossRef]
45. Kennedy AS, McNeillie P, Dezarn WA, et al. Treatment parameters and outcome in 680 treatments of internal radiation with resin ^{90}Y-microspheres for unresectable hepatic tumors. *Int J Radiat Oncol Biol Phys*. 2009;74(5):1494-1500. [CrossRef]
46. Lam MG, Louie JD, Iagaru AH, Goris ML, Sze DY. Safety of repeated yttrium-90 radioembolization. *Cardiovasc Intervent Radiol*. 2013;36(5):1320-1328. [CrossRef]
47. Piana PM, Gonsalves CF, Sato T, et al. Toxicities after radioembolization with yttrium-90 SIR- spheres: incidence and contributing risk factors at a single center. *J Vasc Interv Radiol*. 2011;22(10):1373-1379. [CrossRef]
48. Pan CC, Kavanagh BD, Dawson LA, et al. Radiation-associated liver injury. *Int J Radiat Oncol Biol Phys*. 2010;76(3)(suppl):S94-100. [CrossRef]